Mesopause Region Temperatures over Collm (51.3° N, 13° E)

G. Stober, Ch. Jacobi, D. Kürschner

March 9, 2006

Zusammenfassung

Seit August 2004 wird am geophysikalischen Observatorium Collm (51.3°N, 13°E) ein SKiYMET Meteor-Radar betrieben. Dieses liefert seitdem kontinuierliche Temperaturwerte und Windmessungen. Die Grundlage des Messverfahrens stellt ein stetiger Fluss von Meteoren dar, die in einer Höhe von 75-105 km verglühen. Aus den mit dem Radar bestimmten Positionen der Meteore können Temperaturen in der Mesopausenregion abgeschätzt werden. Für die Darstellung des Jahresganges wurden Tagesmittelwerte genutzt. Dabei tritt im Sommer ein Temperaturminimum mit ca. 170 K auf. Im Winter ist die Situation durch Temperaturen von 205 K und starker planetarer Wellenaktivität gekennzeichnet. Desweiteren konnte eine Klimatologie für die ganz-, halbtägigen und 8-stündigen Gezeiten erstellt werden.

Abstract

Since August 2004 a SKiYMET meteor-Radar is operated at the geophysical Observatory Collm, Germany (51.3°N, 13°E). The radar provides a continuous time series of temperature and wind measurements. The bases for this method is a steady flux of meteors entering the earth's atmosphere. In an altitude between 75-105 km they form a cylindrical plasma trail, which reflects radar signals. Hence the system can determine the positions of the meteors, which are used to estimate mesopause region temperatures. For the diagram of the seasonal change we used daily mean temperatures. The summer shows a temperature minimum with 170 K. During the Winter we observed temperatures about 205 K and a stronger planetary wave activity. Another part was the generation of a climatology for the diurnal, semidiurnal und terdiurnal tide.

1 Introduction

Meteoroids entering the earth's atmosphere form a rapidly expanding plasma trail, the meteor. The life-times of the ionized trails spread from a few hundredths of a second out to several seconds. The backscattered energy depends on the electron density within the trail and the impinging radius of the trail in relation to the transmitting wavelength of the radar. Short after the formation the ambipolar diffusion is the main force for the growth, later on eddy diffusion and recombination becoming more and more important. Hence, we can only use underdense meteors in our analysis, because their half decay times are short enough to neglect other processes. The advantage of this method is, that it is independent of the weather conditions, almost all optical methods suffer from (Lidar or OH-emission). The continuous time series allows an investigation of planetary waves. The radar provides the possibility to measure the typical seasonal variation of temperature and mean wind, including estimates of tidal activity. Thus the radar covers the detection of the main time scales of wave activities in the mesopause region from the long period free rossby waves to the external powered tides.

2 Experimental Setup

The radar consists of three main parts, the transmitting antenna, the receiver antenna array and the receiving/digitizing unit. The antennas are able to detect meteors in the complete hemisphere above the radar. This is a major difference to other meteor-radars, which have a radar beam in a certain direction of the sky. The vertical Yagi antenna design used by the SKiYMET transmits and receives radio waves and echoes out of the whole upper hemisphere. The receiver array is installed in horizontal plane with a 7° slope to operate well. The position of the transmitter is placed outside the array field. The digitizing unit is placed in a small air conditioned building close to the array, typically 70 m away.
The arrangement of the receiving antennas is important for the evaluation of the position. The distance of 2 and 2.5 λ (λ wavelength of the transmitter)

is necessary to reduce the blind areas of the SKiYMET. A closer look at the detected meteors in the x-y plane reveals an eye-like structure (Fig. 1 and 2). In the empty regions the radar was not able to determine the position of the meteor. In the center directly above the array the received phase differences at the antennas are too small and in the ohter empty areas the unambiguous estimation of the distance can not be achieved due to the pulse repetition frequency length (PRF 2144 Hz) of the transmitter. For a good estimate of temperature and wind the exact knowledge of position is very important in order to guarantee the accuracy of the measurement.
The digitizing unit in the air conditioned building consists of 5 receivers, one for each antenna and a UNIX operated Computer for the data analysis. Here the incoming signals are checked if they are real meteor events or not. There is an additional test to separate underdense and overdense meteors. This is achieved through analyzing the different pulse shapes (Fig. 3 and 4) of the two meteor event species. A comparison of the phase delay between the receiver antennas provides the information to evaluate the position. After passing further tests (Hocking et al. [2001]) the identified meteors are stored with all the measurable characteristics in mpd-files on hard disk.

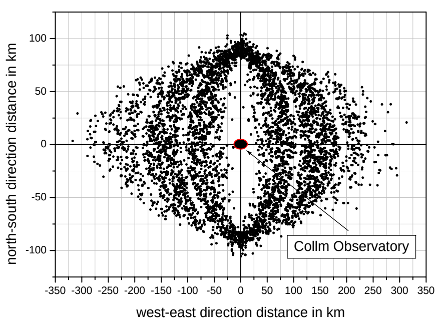

Figure 1: Projection of meteors in the x-y plane detected by the radar during 24 h on 11th November 2004. The gaps result from the problems to determine unambiguously the position of the meteor.

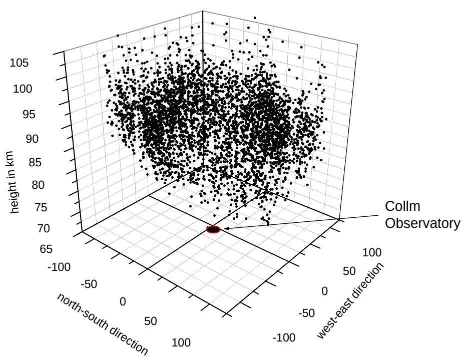

Figure 2: Illustration of the three dimensional meteor cloud used to estimate the temperature for the peak height of the meteor flux on 11. November 2004.

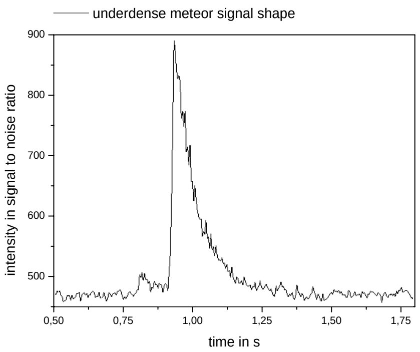

Figure 3: Typical signal shape for an underdense meteor; the sudden jump to the maximum and the exponential relaxation enabling the radar to separate underdense from overdense.

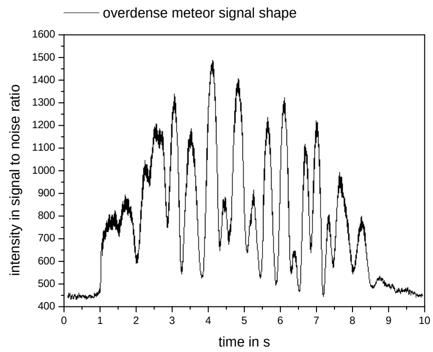

Figure 4: Example of an overdense meteor plot of intensity vs. time detected by a meteor radar. The intensity oscillation is caused by echo interferences.

3 Theory

Jones and Jones [1990] simulated the process of the trail formation and extension, assuming that in the early stage of the quickly formed trail the ambipolar diffusion coefficient is the main force for the growing of the trail and the decay of the electron density. The sudden decay of the ionization level from the maximum to the half amplitude, typical values for $\tau_{1/2}$ are 0.01 to 0.5 seconds, is used to determine the half decay time,

$$A(t) = A_0 e^{-\frac{16\pi^2 D_{amb} t}{\lambda^2}} = A_0 e^{-ln2 \frac{t}{\tau_{1/2}}} \quad , \tag{1}$$

where $A(t)$ is the received field strength at time t, A_0 is the maximum amplitude at $t = 0$, $\tau_{1/2}$ is the half decay time and D_{amb} is the ambipolar diffusion coefficient. By measuring the half decay time the parameter D_{amb} can be estimated,

$$D_{amb} = \frac{\lambda^2 ln2}{16\pi^2 \tau_{1/2}} \quad . \tag{2}$$

The dependence of atmospheric pressure and temperature was then described by the expression;

$$D_{amb} = k_{amb} \frac{T^2}{p} \quad . \tag{3}$$

The constant k_{amb} is related to the main ionic constituent in the plasma trail (Hocking et al.,[1997]). The first step is to remove the pressure parameter using the barometric height formula,

$$p = p_0 e^{-\int_0^z \frac{mg}{kT} dz'} \quad . \tag{4}$$

There we found k as the Boltzmann constant, m is the molecular mass of the gas mixture ($m = 28.8\ u$) and g is the acceleration due to gravity of the meteor peak height (approximately $g = 9.47\ m/s^2$). For this height we define the vertical coordinate z as the altitude of peak meteor activity. In the next step the model of an isothermic atmosphere is replaced by the assumption of a linear temperature gradient. Using (5) and (6) lead us to (7) and applying the natural logarithm to the formula gives us the following connection,

$$T = T_0(1 + \alpha z') \quad , \tag{5}$$

$$\alpha = \frac{1}{T_0} \frac{dT}{dz} \quad , \tag{6}$$

$$lnD_{amb} = lnk_{amb} + 2lnT_0(1 + \alpha z) - lnp_0 + \frac{mg}{kT_0} \int_0^z \frac{1}{(1 + \alpha z')} dz' \quad , \tag{7}$$

where α is the vertical temperature gradient in the height z. The new vertical coordinate z' is zero at the maximum flux of meteors and measures the distance from this altitude. After this all constants are removed by applying the vertical derivation to the equation. The vertical dependence of D_{amb} was shown by Hocking et al.,[1999],

$$\frac{d}{dz} lnD_{amb}|_{\ z=0} = 2\frac{d}{dz} lnT_0(1 + \alpha z) + \frac{mg}{kT_0} \frac{d}{dz} \int_0^z \frac{1}{(1 + \alpha z')} dz'|_{z=0} \quad . \tag{8}$$

Solving the integral lead to the following expression;

$$\frac{d}{dz} lnD_{amb} = 2\alpha + \frac{mg}{kT_0} \quad . \tag{9}$$

In equation (9) we used the fact that the introduced vertical coordinate z, which was zero at the height of peak activity, is leading to the given terms. Lastly the term $\frac{d}{dz} ln\ D_{amb}$ is estimated by a best fit line S_m. From this the final formula for temperature can be extracted,

$$\frac{1}{S_m} \propto \frac{d}{dz} ln\ D_{amb} \quad , \tag{10}$$

$$T_0 = S_m \Big(2\frac{dT}{dz} + \frac{mg}{k} \Big) \quad . \tag{11}$$

Temperature gradient model

Equation (11) gives the relation between the known parameters m (mean molecular mass), g (acceleration due to gravity), k (Boltzmann constant), S_m (the best fit line) and the unknown vertical temperature gradient $\frac{dT}{dz}$. Ignoring the temperature gradient will increase the absolute error to a value of about 15 K. The first models which were introduced, were based on rocket measurements and the CIRA 86 climatology and showed the seasonal vertical movement of the mesopause. So the model had slightly positive values in the summer. During the winter months the gradient remained almost constant with approximately -1.5 K/km. But the structure was too simple and recent investigations with Lidar and other methods revealed a more detailed variability. Adding these results a new model was created (Fig. 5). The last interesting point is the best fit line. In the analysis algorithm a linear Gaussian fit is used. But there are several other fits possible. For instance Hocking et al. [2001] suggested a polynomial fifth order fit in his procedure. A compari-son of both methods is shown in (Fig. 6). The fifth order polynomial seems to be more stable in the summer months. However at the moment there is no analytical approach to show, wheather a linear fit or polynomial fit should be taken as the best. Probably a χ^2-test will give a better base for a decision, which is a task for future investigations.

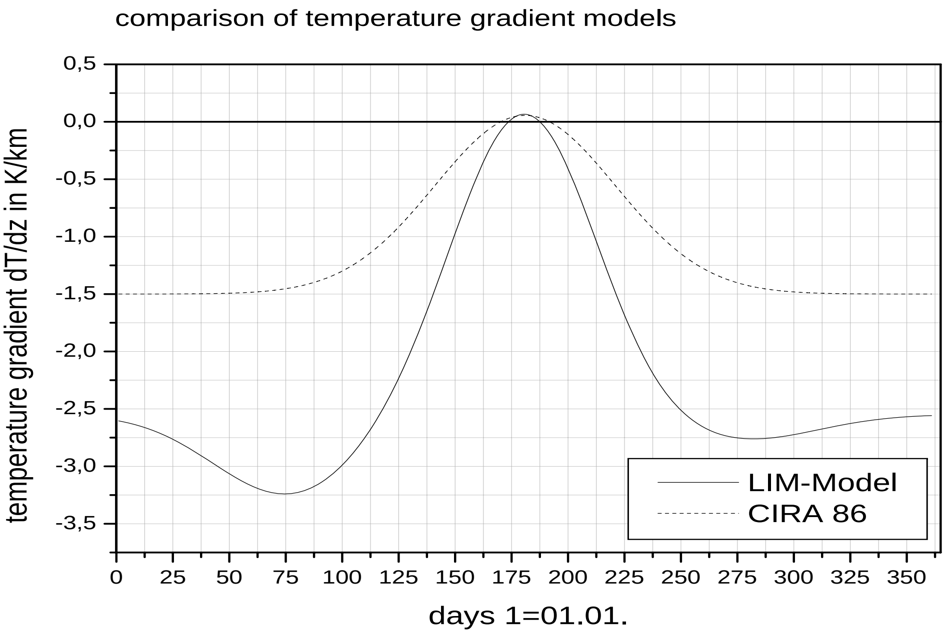

Figure 5: The plot shows two different empirical temperature gradient models. There are several more with more or less similar behavior.

4 Filter and Bias Adjustment

Before the calculation procedure can be used, some adjustments to the raw-data are necessary. In the files all meteor events are stored, means that unambiguous meteors are included. This kind of data has to be rejected. In addition to this all data above a range of 400 km, a height less than 70 km or above 108 km and decay times smaller than 0.025 s or greater than 0.5 s are rejected. Another exclusion criterion is the demand that decay times greater than 0.1 s above a height of 96 km and less than 0.05 s in 84 km are rejected. The remaining data is now grouped into several bins of the quantity $log\frac{1}{\tau_{1/2}}$ (0.5-0.7), (0.7-0.9), (0.9-1.1), (1.1-1.3), (1.3-1.5) and (1.5-1.7). For each of these bins a median filter is applied and all points outside the 2σ interval are removed (Fig. 7).

The final process in the analysis is the bias adjustment. This is a correction due to the various instrumental errors. Considering a large group of meteors with the same decay time, there is a spread in the measured heights. The limited accuracy of the instrument can be approximated by a Gaussian distribution $e^{-(h-h_r)^2/(2\sigma_r^2)}$. On the other hand a closer look at the height dis-

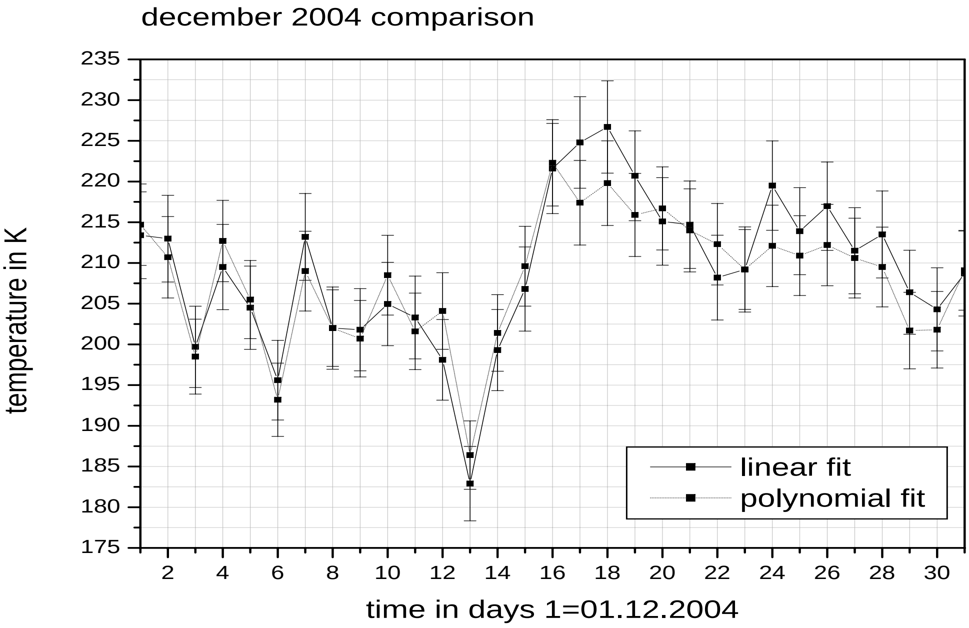

Figure 6: The comparison of the two fit line reveals the small differences between them. Both plots show daily means with their statistical errors.

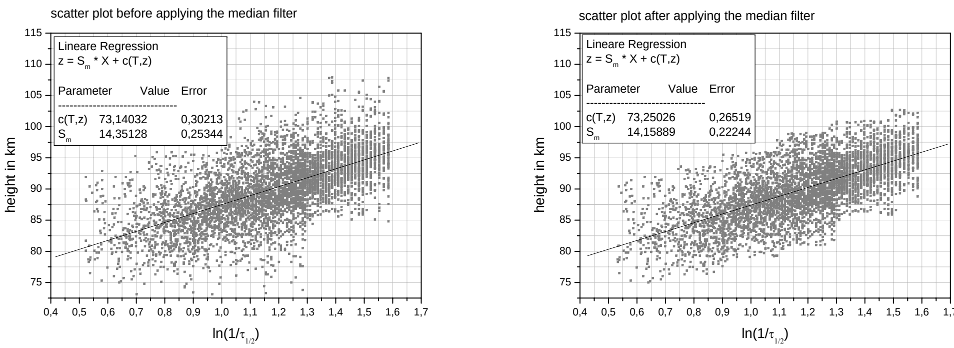

Figure 7: Typical scattered plots of height vs. inverse decay time compared before and after applying the median filter. The picture includes 24 hours of data.

tribution of all remaining meteors reveals a flux peaking at around 90 km, for a radar operating with 32-50 MHz. The distribution can be approximated with a Gaussian function of the form $e^{-(h-h_p)^2/(2\sigma_p^2)}$ (Fig. 8). As a consequence the expected value is given by the weighted average of the product of these two distributions,

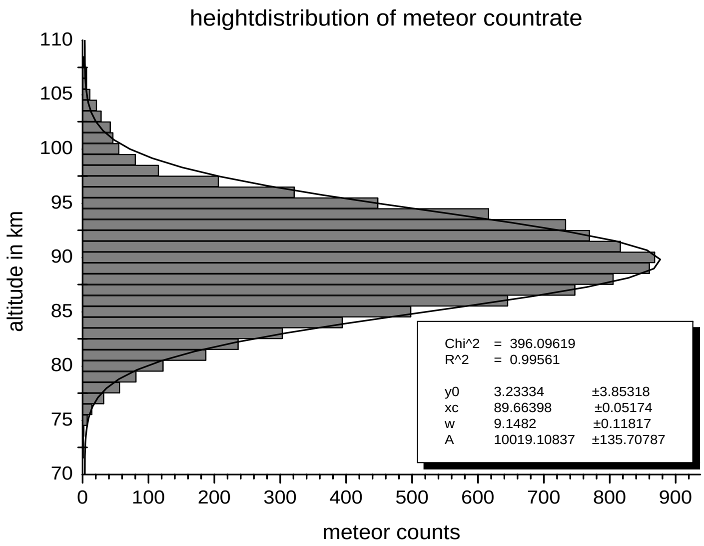

Figure 8: Measured height distribution with 2 km gates and a Gaussian best fit line. The peak altitude of the meteor flux is found at about 90 km.

$$h_{measured} = \frac{\int_{-\infty}^{+\infty} h e^{\frac{-(h-h_r)^2}{2\sigma_r^2}} e^{\frac{-(h-h_p)^2}{2\sigma_p^2}}}{\int_{-\infty}^{+\infty} e^{\frac{-(h-h_r)^2}{2\sigma_r^2}} e^{\frac{-(h-h_p)^2}{2\sigma_p^2}}}. \tag{12}$$

In the equation there are only two unknown values. One of them is the standard deviation of the instrumental error σ_r, which is estimated by the angular resolution of approximately 2° and the pulse repetition frequency length. This leads to values of 2-3 km. Actually a mean value of 2.1 km shows good results. The second unknown value is the true height. Therefore equation (12) has to be inverted to calculate the value of h_r. The parameter h_p equals the median of the height distribution and can be directly taken from the data, as well as the standard deviation σ_p. Typically the ascend of our slope is increased by 30% applying the adjustment.

5 Results

On the basis of the 2005 data and using the described procedure reliable absolute temperature estimates were calculated. The following analysis is based on daily mean values, which are slightly biased by the daily oscillation of the meteor flux. The error bars shown include the statistical error. These errors are derived easily from the linear fit. The error of the temperature gradient model is not known, but a comparison with other measurements lead to a good coincidence within a total error of 8-10 K. The plots show the typical seasonal temperature course for the mesopause region of 90 km altitude (Fig. 9). The Geminid meteor shower in December (09.-16.12.) results in a reduced temperature value, because of the lower height of meteor peak activity with 87 km. This is the first complete seasonal climatology for this atmospheric region at the Collm Observatory.

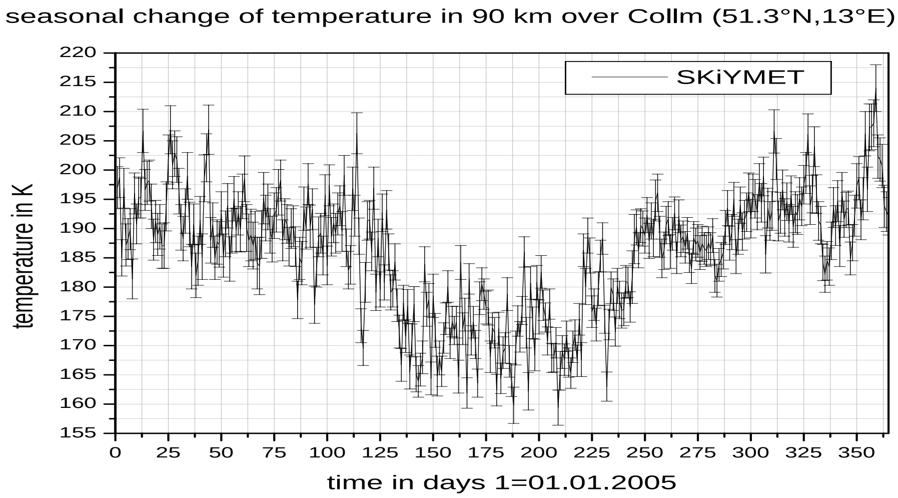

Figure 9: Graph of the daily mean temperature in 90 km altitude including statistical errorbars. The plot shows two significant planetary waves. The first event happened in the summer around day 200 (begin of July) and showed an increased temperature of 20 K. The second interesting event is the Geminid meteor shower in December. There the temperature drops by 10-15 K.

The final step was the creation of a routine to detect temperature tides. A first simple strategy would lead to take hourly data and running the standard analysis. Hence, the temperature estimates are only found with an accuracy of 30-40 K. Indeed it is possible to accumulate all meteors of the same hour over 7 days (Singer [2005]). This process has two advantages: the data base is enlarged and the temperature gradient fluctuations are reduced. The price to pay for a hourly resolution is the loss of long term oscillations. In fact the procedure smooths the temperature profile. For the tide this process is not important, because of the stability of the tidal phase during the 7 day accumulation time. This enables us to create a time series with hourly means and one day shift allowing an investigation with a Fourier analysis. The amplitudes received by this method are shown in the following tidal climatology (Fig. 10).

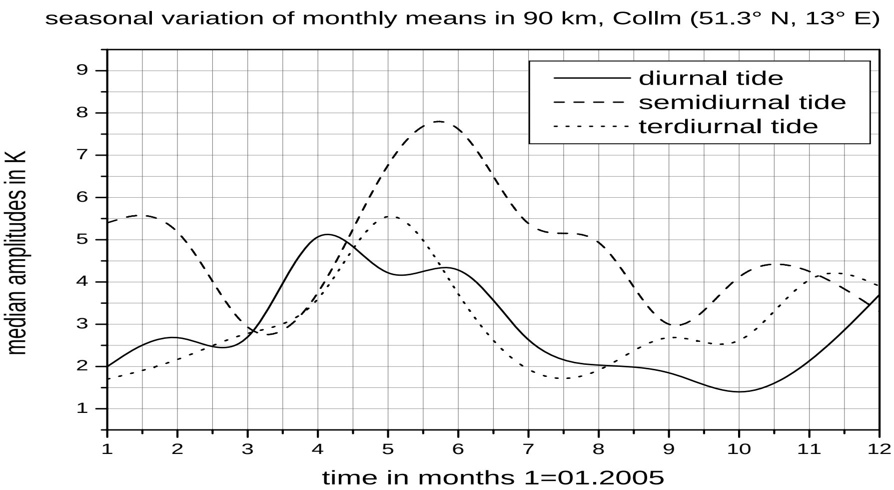

Figure 10: The graph gives an impression of amplitudes for the diurnal, semidiurnal and terdiurnal tide. The amplitudes were calculated with monthly accumulated data.

6 Conclusion

At Collm Observatory, a SKiYMET meteor radar has been installed in summer 2004, measure winds and ambipolar diffusion coefficients in the mesosphere/lower thermosphere region. After more than one year of measurements, first seasonal climatologies of the relevant parameters can be constructed. Here we focus on temperatures, which are derived from the vertical gradient of the ambipolar diffusion coefficient under the assumption of a known temperature gradient profile.
The results show that daily mean temperatures can be estimated with the radar. In addition, estimates of temperature tides (8, 12, and 24-h component) can be calculated on the basis of at least seven days of hourly data. The results of both mean temperatures and tidal amplitudes show good correspondence with those given in the literature.

Acknowledgments

The support of the department of Meteorology Leipzig is recognized. Special thanks go to K. Fröhlich for her advices, guidance and help, during the work. Also the technical support and maintenance of the radar by D. Kürschner is outlined and emphasized. Thanks also to Ch. Viehweg for accompanying me to St. Petersburg.

References

Hocking W.K., Thayaparan T. and J. Jones, Meteor decay times and their use in determining a diagnostic mesophereic temperature-pressure parameter: methodology and one year of data, *Geophysical Research Letters*, Pages 2977-2980, 1997

Hocking W.K., Temperatures using radar-meteor decay times, *Geophysical Research Letters*, Pages 3297-3300, 1999

Hocking W.K., B. Fuller, B.Vandepeer, Real-time determination of meteor-related parameters utilizing modern digital technology, *Journal of Atmospheric and Solar-Terrestrial Physics 63*, 2001

Hocking W.K., W. Singer, J. Bremer, N.J. Mitchell, P. Batista, B. Clemesha, M. Donner, Meteor radar temperatures at multiple sites derived with SKiYMET radars and compared to OH, rocket and lidar measurements, *Journal of Atmospheric and Solar-Terrestrial Physics 66*, 2004

Singer W., R. Latteck, P. Hoffman, B.P. Williams, D.C. Fritts, Y. Murayama and K. Sakanoi, Tides near the Artic summer mesopause during the MaCAWE/
MIDAS summer program, *Geophysical Research Letters*, 2005

Jones, W.,and J. Jones, Ionic diffusion in meteor trails, *J. Atmos. Terr. Phys., 52*, 185-191, 1990

Wiss. Mitteilungen
Aus dem Institut f. Meteorologie der Universität Leipzig Bd. 37, 2006